Axon guidance by growth-rate modulation

Duncan Mortimer[a,1], Zac Pujic[a,1], Timothy Vaughan[a,1], Andrew W. Thompson[a], Julia Feldner[a], Irina Vetter[a], and Geoffrey J. Goodhill[a,b,2]

[a]Queensland Brain Institute and [b]School of Mathematics and Physics, University of Queensland, St Lucia, Queensland 4072, Australia

Edited by Charles F. Stevens, Salk Institute for Biological Studies, La Jolla, CA, and approved February 2, 2010 (received for review August 14, 2009)

Guidance of axons by molecular gradients is crucial for wiring up the developing nervous system. It often is assumed that the unique signature of such guidance is immediate and biased turning of the axon tip toward or away from the gradient. However, here we show that such turning is not required for guidance. Rather, by a combination of experimental and computational analyses, we demonstrate that growth-rate modulation is an alternative mechanism for guidance. Furthermore we show that, although both mechanisms may operate simultaneously, biased turning dominates in steep gradients, whereas growth-rate modulation may dominate in shallow gradients. These results suggest that biased axon turning is not the only method by which guidance can occur.

chemotaxis | growth cone | nerve growth factor | neural development | computational neuroscience

For the brain to function correctly, its neurons must be connected correctly, and wiring problems are known to underlie a number of nervous system disorders (1, 2). Some of the most important cues guiding the formation of connections between neurons in the developing nervous system are molecular gradients (3–10). To respond to a gradient cue, an axon must be able both to make a decision regarding gradient direction and then to convert that decision into directed motion (8). Although recent research has addressed the mechanisms involved in the decision-making step (11), how a decision regarding gradient direction is subsequently converted into a change in behavior of the growth cone is largely unknown.

The most obvious mechanism in this regard is immediate and biased turning, whereby the axon tip is more likely to turn up the gradient (or down in the case of repulsive factors) each time the gradient direction is assessed. Such behavior is observed in in vitro assays that examine the response of axons to steep gradients of tropic factors in two dimensions (12–17). However, 3D in vitro assays, which reproduce more closely the conditions of axon growth in vivo, often fail to show consistent turning of axons. Rather, in these assays it tends to be the collective growth of a population of axons that is biased by the gradient (e.g., refs.18–20). Whether immediate and biased turning of axons in response to gradient signals occurs in vivo can be hard to assess, because in any specific situation axons are likely to respond to a combination of many different types of guidance cue. Here, we show that asymmetric growth of axons in response to a gradient signal does not require immediate and biased turning, and we identify an alternative mechanism for axonal chemotaxis based on growth-rate modulation. Our data suggest that, although immediate and biased turning and growth-rate modulation may operate together, the former dominates in steep gradients, whereas the latter dominates in shallow gradients.

Results

Lack of Neurite Turning for Explants in Gradients. Previous analyses of neurite outgrowth from explants in 3D collagen gels generally have not included a quantitative analysis of turning. We therefore developed an automated method for measuring turning in explant images using a steerable ridge filter (21) (*Materials and Methods*) that enabled us to label each part of the image objectively as representing turning up or down the gradient. This identification was based on local information for each small region of the image rather than on complete axon trajectories, because the high density of neurite outgrowth made it impossible to reconstruct complete trajectories from our images. From these measurements an overall turning ratio (TR) was defined for each explant that varied between +1 (all turning up the gradient) and −1 (all turning down the gradient), with a zero value representing no net turning (*Materials and Methods*). We validated this method by showing that it is highly correlated with both human assessments of turning in real explant images (Fig. S1) and with explicitly curvature-based measures of turning in simulated explant images for which complete trajectory information was available (Fig. S2).

We then measured how the TR varied with gradient conditions in a dataset of ≈ 2,500 dorsal root ganglion (DRG) explants grown for 48 h in exponentially shaped gradients of nerve growth factor (NGF) in which both the gradient steepness and absolute concentration were varied precisely, as described in ref. 11. Fig. 1 shows examples of explant images and the values of the TRs obtained as a function of gradient conditions. Also shown are the previously determined values of the guidance ratio (GR), which compares the overall growth up the gradient with that down the gradient (11, 22) (*Materials and Methods*). Although some TR values are significantly different from the zero-gradient condition (Table S1), all are close to zero, even when the GR values are strongly positive. Restricting the turning analysis to only a subregion of each image, such as a narrow strip oriented perpendicular to the gradient through the center of each explant, did not change the TR values significantly. Thus, explants can display highly asymmetric neurite growth without strongly biased turning of neurites.

Asymmetric Outgrowth Is Not Explained by a Purely Trophic Response. How is this asymmetric growth possible? In common with axon guidance molecules such as netrin (23) and ephrinA (26), NGF can have both chemotactic (tropic) and growth-promoting (trophic) effects on the same neurites. Therefore one potential explanation for the asymmetric neurite growth we observed in our explants is that the growth of neurites on the side of the explant facing up the gradient is differentially promoted simply because there is more NGF on the up-gradient side. To eliminate this possibility, we exploited the precise and reproducible control over gradient conditions afforded by the collagen gel pump assay (11, 22) and cultured a zigzag pattern of DRG explants in an NGF gradient (Fig. 2*A*). The trophic hypothesis, i.e., that the only influence on the movement of a growth cone is the absolute concentration of ligand it experiences at each moment, independent of how that concentration changes with space or time, predicts that total neurite growth from each side of each explant should be independent of whether that side is facing up or down the gradient and will be determined purely by the ligand concentration at each position (shown schematically in Fig. 2*B*). In contrast, the tropic hypothesis

Author contributions: G.J.G. designed research; D.M., Z.P., T.V., A.W.T., J.F., and I.V. performed research; T.V. contributed new reagents/analytic tools; D.M., Z.P., A.W.T., J.F., and I.V. analyzed data; and D.M., Z.P., T.V., and G.J.G. wrote the paper.

The authors declare no conflict of interest.

This article is a PNAS Direct Submission.

Freely available online through the PNAS open access option.

[1]D.M., Z.P., and T.V. contributed equally to this work.

[2]To whom correspondence should be addressed. E-mail: g.goodhill@uq.edu.au.

This article contains supporting information online at www.pnas.org/cgi/content/full/0909254107/DCSupplemental.

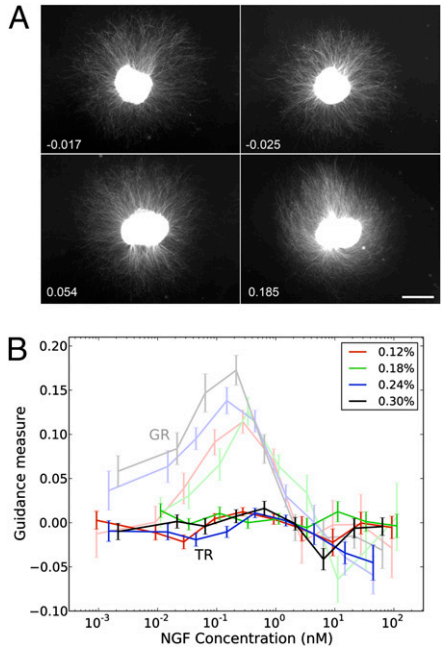

Fig. 1. DRG neurites show little average turning in gradients which produce strongly biased outgrowth. (*A*) Example of DRG explants grown in precisely controlled gradients for 48 h (stained with β3-tubulin), and corresponding TR values. NGF gradient increased upwards in each case. Images at left and upper right are representative and have low turning ratios. The image at lower right is an atypical case with a very high turning ratio. (Scale bar, 500 μm.) (*B*) The *y* axis refers to the values of both the GR and TR. Bright lines show TRs as the background NGF concentration varies; different colors represent the different gradient slopes (defined as fractional change across 10 μm) as shown in the key. Shadowed lines show the previously determined corresponding GRs (11). Some TRs are significantly different from the no-gradient control condition (for *n* and *P* values, see Table S1), but all TRs are small compared with the GRs. At high NGF concentrations there is strong fasciculation and low neurite outgrowth (11), and thus both the GR and TR data become noisier and less reliable. Error bars are SEMs.

predicts that total neurite growth from each side should depend strongly on whether the side is facing up or down the gradient but should be relatively independent of concentration. The amount of neurite growth observed experimentally (Fig. 2*C*) was the same for the explant sides facing up the gradient, even though those sides were at different concentrations, and this growth was significantly greater than for the explants sides facing down the gradient, although for half of these downward-facing explant sides the NGF concentration was higher than for the explant sides facing up the gradient. These data are consistent with the tropic hypothesis but are inconsistent with the trophic hypothesis.

Delaying Gradient Application Does Not Produce Turning. A second possible explanation for biased outgrowth without immediate and biased turning is that most turning occurs before neurites leave the explant and thus is invisible to our turning-ratio analysis. To test this hypothesis, we delayed application of the NGF gradient for up to 24 h after explant plating to allow the neurites time to emerge from the explant (for details see ref. 11). We then analyzed the pattern of neurite turning 48 h after plating. It might be expected that a gradient applied to already visible neurites initially growing in an undirected manner would cause an obvious turn. However, when we analyzed turning in these explants, we found no change in the TR with time delay, and again the turning response was small in magnitude (Fig. S3). Thus, initial turning of neurites inside the explant cannot explain the lack of strong turning after they have emerged from the explant.

Lack of Turning Is Not Explained by Straightening of Neurites by Tension. A third possible explanation for the lack of strong turning in explant images at 48 h is that neurite trajectories were indeed curved as they grew but subsequently straightened because of neurite tension (27). To test this hypothesis, we performed time-lapse imaging of neurite growth from explants in gradients in collagen gels and compared the actual path taken by the neurite tip over several hours with the final trajectory of the neurite (Fig. S4). There was little difference between the instantaneous and final trajectories, demonstrating that later straightening of trajectories does not explain the lack of strong turning seen in our experiments.

If Immediate and Biased Turning Is Present, It Can Be Detected. A fourth possible explanation is that there is underlying immediate and biased turning, but our method for quantifying turning is not sensitive enough to detect it. To test this possibility, we analyzed simulated explant images which we knew contained immediate and biased turning. We recently have shown that the bias in axonal response to gradients as a function of gradient parameters is well matched by a Bayesian model for how growth cones combine noisy receptor-binding measurements to make a decision regarding gradient direction (11). However, that model made no commitment as to how this decision was translated into a change in behavior of the growth cone. We therefore extended this model by coupling it to a biased random-walk model of neurite growth. Besides moving forward, at each timestep each neurite tip made a turn up the gradient with a probability related to the signal-to-noise ratio (SNR) calculated from the Bayesian model (for details, see *Materials and Methods*). We used this model to generate artificial explants with properties of neurite growth and image noise matched to our experimental data (Fig. 3*A*). The GR and TR for these artificial explants then were measured using the same *n* values and SNR conditions used for the experimental data. The simulated GR curves match well with the experimental data (compare Figs. 1 and 3*B*). However, the simulated TR values are much larger than those measured experimentally. Thus, when immediate and biased turning was known to be present, our method for quantifying turning was able to detect it. Because we had complete knowledge of the underlying neurite trajectories used to generate the simulated explants, we also used these simulations to show that the TR values are strongly correlated with a measure explicitly based on curvature (Fig. S2).

Growth-Rate Modulation Explains These Data. Because the model based purely on immediate and biased turning failed to reproduce our data, we considered a different model for how a decision regarding gradient direction is converted to directed motion. The immediate and biased model can be imagined as representing a growth cone making a comparison in ligand receptor binding between its left and right side and then immediately turning left or right accordingly. We now imagined that, instead, the growth cone makes a comparison along its front-to-back axis and then modulates its speed of growth relative to the SNR calculated from the Bayesian model (*Materials and Methods*). At each timestep the growth cone also turns slightly, but the direction of this turn is assumed to be random and unrelated to the gradient direction. Artificial explants grown with this mechanism under the same conditions as those used experimentally (Fig. 3C) appear visually similar to explants simulated with the explicit turning model (Fig. 3*A*). However, applying the GR and TR analyses as before revealed that both the GR and the TR now match the experimental data much more closely (Fig. 3*D*). In particular, even for gradient conditions for which explants show a large GR value, the TR value is small. A more direct comparison of the GR and TR values produced experimentally with those produced from the two different models confirms that the experimental data match the growth-rate modulation much more closely than the turning model (Fig. 3*E*). Although in the growth-rate model the

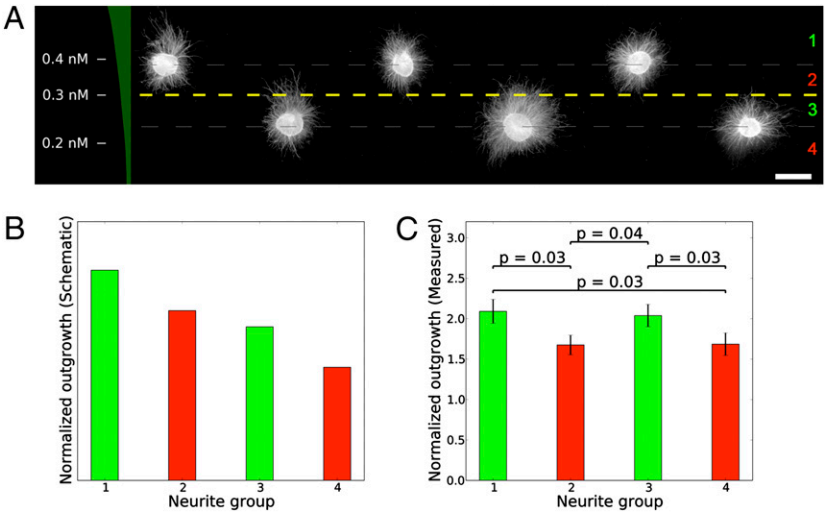

Fig. 2. Trophism does not explain biased outgrowth in a gradient. Culture dishes (35 mm), each containing a zigzag pattern of six DRG explants, were printed with an NGF gradient of 0.3% fractional change across 10 microns, with an absolute concentration of 0.3 nM at the line equidistant between the two rows of explants. (*A*) Reconstruction of DRG explants in one plate (NGF gradient increasing upwards). (Scale bar, 1 mm.) The yellow dashed line marks the center of the zigzag pattern, and the gray dashed lines mark the approximate centers of the two sets of explants. On the left, the shape of the NGF gradient is shown schematically, along with accompanying estimates of the actual concentration present at different positions in this gradient. On the right, the red and green numbers label the groups of neurites whose outgrowth are compared. (*B*) If the amount of outgrowth from each side of an explant is purely a function of absolute concentration, then the amount of outgrowth should be ordered as group 1 > group 2 > group 3 > group 4 (shown schematically), because the average concentration decreases between each of these regions. On the other hand, if the amount of outgrowth is determined by the direction of the gradient vector, the ordering should be group 1 ≈ group 3 > group 2 ≈ group 4; that is, growth should depend more on the direction of neurite growth relative to the gradient than on absolute concentration. (*C*) Measured outgrowth for the four groups of neurites labeled in *A*. Group 1 has the same growth as group 3, group 2 has the same growth as group 4, and group 2 has significantly lower outgrowth than group 3 despite being at a slightly higher NGF concentration, ruling out the trophic hypothesis. n = 93–95 per group, averaged over three separate experiments. P values shown are from a t test. The two green bars are not significantly different, nor are the two red bars.

steps up the gradient tend to be slightly longer than the steps down the gradient, it nonetheless is equally probable that a neurite segment chosen at random will be curving away from the gradient as curving toward it. This fact is illustrated by simulation in Fig. 3F and is proved mathematically in the *SI Text* (see also Figs. S5 and S6).

Which Guidance Strategy Dominates Depends on the Steepness of the Gradient. The above experimental and computational results suggest that neurites respond to shallow gradients in 3D collagen gels primarily by varying their growth rate rather than by immediate and biased turning. This finding contrasts with the strong turning re-

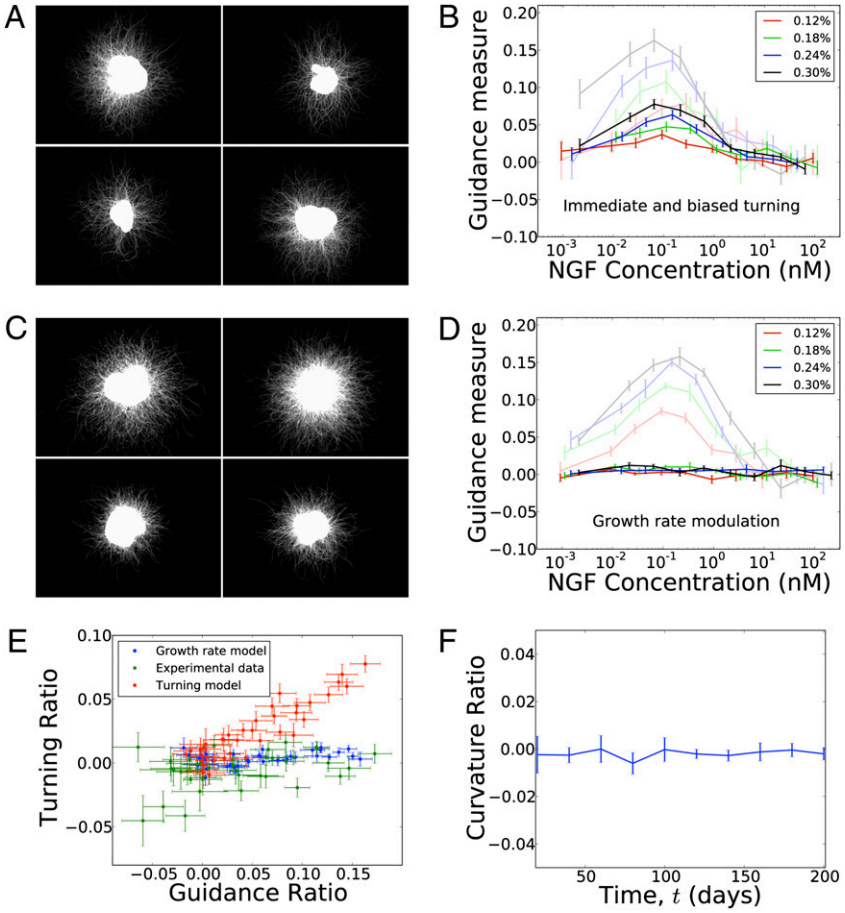

Fig. 3. A computational model of growth-rate modulation matches the data better than a model of turning. (*A*) Examples of explants produced by the immediate and biased turning model. (*B*) GR (shadowed lines) and TR (bright lines) values produced by the immediate and biased turning model. When this figure is compared with Fig. 1, it can be seen that the GR values match well, but the TR values in the model are much larger than those seen experimentally. (*C*) Examples of explants produced by the growth-rate modulation model. (*D*) GR and TR values produced by the growth-rate modulation model. Both the GR and TR values match the experimental data (Fig. 1). (*E*) Correlation between GR and TR values for the experimental data and the two models, confirming that the growth-rate modulation model fits the experimental data much more closely than does the immediate and biased turning model. There is one point of each color for each of the 38 combinations of gradient steepness and concentration investigated experimentally. (*F*) Simulated explants generated using the growth-rate modulation mechanism fail to show significantly more neurites curving in the direction of the gradient than away from it, even at very long timescales (100 times longer than those used in panels *A* and *C*). Each point shows mean ± SEM, n = 50 explants; curvature ratio is defined in Fig. S2).

sponse observed for neurites on 2D substrates with steep gradients (12–17). But do neurites in steep gradients also modulate their growth rate depending on whether they are growing up or down the gradient? First we confirmed that, as observed for other types of neurons (14), superior cervical ganglion (SCG) neurites respond to gradients of NGF in the conventional pipette or growth cone turning assay by turning (Fig. 4 *A* and *B*). We then adapted this assay to compare the growth rate of individual neurites when the pipette was placed directly in front of the growth cone with the growth rate when the pipette was placed directly behind the growth cone (*Materials and Methods*). Growth rates were indistinguishable in the two conditions (Fig. 4 *C* and *D*), suggesting that the strategy of growth-rate modulation for chemotaxis observed in shallow gradients in 3D collagen gels does not generalize to the steep gradients of the 2D pipette assay.

Finally, we asked whether the difference in chemotactic strategy is caused by the parameters of the gradient or the nature of the substrate. We did so by developing a version of the pipette assay in a 3D collagen gel, thus changing the gradient parameters without changing the substrate (*Materials and Methods*). In this case, turning of SCG neurites toward the pipette was observed (Fig. 4 *E* and *F*). Thus, gradient steepness, rather than the nature of the substrate, determines the chemotactic strategy used.

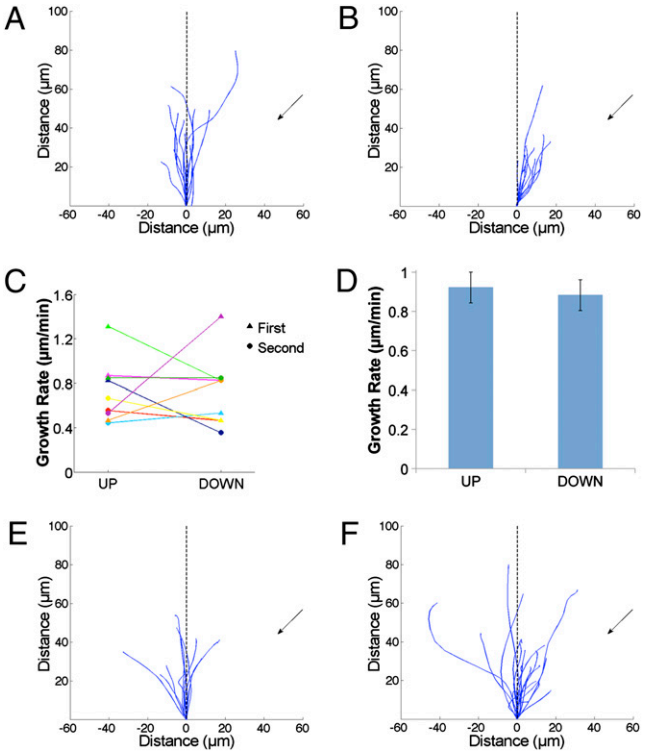

Fig. 4. Turning dominates growth-rate modulation in steep gradients. (*A* and *B*) Confirmation that rat SCG neurites turn in response to gradients of NGF in the pipette assay. (*A*) Traces of individual neurite trajectories in the control (PBS gradient) condition. Arrow shows direction of the pipette (*Materials and Methods*). $n = 12$, mean turning angle = −2.1°. (*B*) Neurite traces for 10 μM NGF in the pipette. $n = 10$, mean turning angle = 15.6°. The NGF and control conditions are significantly different ($P = 0.003$, Kolmogorov-Smirnov test). (*C* and *D*) Comparison of neurite growth rates with the pipette directly in front of the growth cone and with the pipette directly behind the growth cone. (*C*) Paired data ($n = 9$): each line shows the growth rates for the same neurite growing up or growing down the gradient. "First" and "second" refer to the order in which the gradients were presented to each axon. Gradient direction has no effect on growth rate ($P = 0.92$, paired *t* test). (*D*) Overall comparison of growth rates (unpaired data, $n = 11$ up, 14 down, $P = 0.36$, unpaired *t* test). (*E* and *F*) SCG neurites turn in NGF gradients produced from a pipette in 3D collagen. (*E*) PBS control. $n = 10$, mean turning angle = $-6.8 \pm 6.2°$ (not statistically different from zero, $P = 0.3$, one-sample *t* test). (*F*) NGF (10 μM) in the pipette. $n = 18$, mean turning angle = 10.3° (mean is statistically different from zero, $P = 0.04$, one-sample *t* test). The distributions of *E* and *F* are significantly different ($P = 0.01$, Kolmogorov-Smirnov test.)

Discussion

It often is assumed that the only way to determine unambiguously if a growth cone has detected a gradient is for the growth cone to display immediate and biased turning in response to that gradient. We have shown that growth-rate modulation is an alternative read-out mechanism that can be important under certain circumstances. Thus, although immediate and biased turning certainly suggests guidance, a lack of such turning does not definitively imply no guidance. It has been discussed previously that axons sometimes grow further when moving straight up a gradient than when moving either straight down a gradient or on a uniform concentration (24–26). Our growth-rate modulation model is consistent with these proposals but is expressed more precisely as a computational model of axon movement in two dimensions. Furthermore, we have shown that this model is quantitatively consistent with the behavior of axons grown under precisely controlled gradient conditions.

Why might gradient steepness be a key factor in determining which read-out mechanism dominates? We suggest a crucial issue is that immediate turning requires comparing concentrations between the left- and right-hand sides of the growth cone, a distance that is generally only a few microns. On this scale the differences in receptor binding induced by a shallow ligand gradient can be extremely small, particularly for low ligand concentrations (11). Thus, under these circumstances, a decision to turn left or right will be very unreliable. In contrast, a growth-rate modulation method potentially allows comparisons of concentrations over much longer distances. The comparison could be between the growth cone and regions of the axon shaft many tens of microns behind the growth cone, or indeed between the growth cone and the soma itself. This increase in distance relative to the width of the growth cone dramatically increases the difference in concentration to be detected and thus the fidelity of the guidance decision. However, in this case, a read-out in terms of immediate and biased turning is no longer possible, leaving a change in growth rate as the obvious alternative. For the measurements we have made so far, it is not possible to determine this distance, because it is combined with other unknown biological variables in the proportionality constant in our expression governing how response varies with gradient parameters [Eq. **2**] (*Materials and Methods*).

Immediate and biased turning and growth-rate modulation need not be exclusive mechanisms. The fact that a small but significant TR is seen in our explant data is consistent with the idea that growth cones still are attempting to turn in response to the gradient but do so very unreliably, as expected from the very small change in concentration across their width. Growth-rate modulation then is the dominant mechanism. In contrast, in the pipette assay, where the gradient is highly localized, the difference in concentration between the growth cone and more distal parts of the axon is independent of gradient direction, and so no growth-rate modulation would be expected. A similar transition between gradient-detection strategies could apply as growth cone size varies with species and/or assay conditions. For large growth cones, biased turning may be a sufficiently reliable response, whereas for small growth cones growth-rate modulation may become more effective. Overall, we suggest that immediate and biased turning and growth-rate modulation work together to guide axons to their targets, but we predict that the relative importance of each mechanism in any particular case will be determined by the parameters of the gradient.

Materials and Methods

Printing Assay. DRGs from P2 rat pups were dissected into ice-cold Leibovitz's medium, trimmed of excess axonal tissue, and digested with 0.25% trypsin for

10 min. DRGs then were embedded in collagen, and an NGF gradient was printed as described elsewhere (11, 22). Briefly, 750 μL of 0.2% type I rat tail collagen was allowed to set in a 35-mm Petri dish. Six DRGs then were embedded in 750 μL of collagen which overlaid the first layer. A Nanoplotter (Gesim) then was used to print gradients of NGF of varying steepness. For the zigzag experiment, the DRGs were positioned on either side of a line at which the NGF concentration was 0.3 nM and steepness was 0.3% across 10 μm (Fig. 2*A*). After 2 days incubation at 37 °C and 5% CO_2, the DRGs were immunostained for β3-tubulin and photographed using ApoTome imaging with a Zeiss Z1 microscope.

Measurement of Neurite Outgrowth and Explant Asymmetry. Outgrowth asymmetry was quantified using the guidance ratio GR = (H − L)/(H + L), *H* and *L* being the number of neurite pixels on the high and low ligand concentration sides of the explant, respectively (11). Total outgrowth was calculated as the total number of neurite pixels (i.e., H + L) divided by *E*, the number of pixels in the explant. For the zigzag experiment, outgrowth on each side was calculated as H/E and L/E, respectively.

Time-Lapse Imaging of DRG Neurites. DRGs were subjected to the printing assay as described above (0.3%/0.3 nM gradient of NGF). After 24 h of growth in an incubator at 37 °C and 5% CO_2, neurites were photographed using phase-contrast microscopy with a 20× objective on a Zeiss Z1 microscope at 10-min intervals for up to 6 h. The position of the growth cone at each interval then was marked using ImageJ (http://rsbweb.nih.gov/ij/download.html) and compared with the trace of the resulting axon.

Quantification of Neurite Turning. Because of the high density of neurite outgrowth from our explants, it was not possible to reconstruct individual neurite trajectories reliably. Thus, to each pixel we assigned a turning value corresponding to a neurite in the micrograph and used these values directly. In particular, a steerable ridge filter (21, 28) was applied to the nonexplant region of image to identify pixels corresponding to neurites and to estimate the orientation angle of the associated neurite (for more details, see *SI Text*). For each neurite pixel we determined the difference vector of smallest magnitude between each of the two opposing unit vectors lying parallel to the neurite orientation angle and the unit vector pointing from the center of the explant to the neurite pixel. We classified each neurite pixel as turning up or down the gradient according to the sign of the component of this vector pointing up the ligand gradient (Fig. S1*A*). The turning ratio of the explant then was calculated by TR = (U − D)/(U + D), *U* and *D* being the number of pixels turning up-gradient and down-gradient, respectively.

To confirm that this measure was consistent with human estimates of the degree of turning in explant images, seven observers assigned each member of a selected corpus of 188 explant images an integer score ranging from −2 (strong downward turning) to +2 (strong upward turning), with zero representing no turning. There is good correlation between the two sets of values (Fig. S1*B*). Furthermore, we confirmed that for simulated explants in which substantial turning is present, the turning ratio measure is highly correlated with a measure based explicitly on the curvature of individual neurite trajectories (Figs. S2 and S5).

Explant Simulations. Simulating a single explant involved three steps: (*i*) generating a mock explant body and seeding it with neurite outgrowth sites, (*ii*) generating neurite trajectories according to the growth models of interest, and (*iii*) compositing the explant body with the neurite trajectories (with a degree of imaging noise) to generate a final simulated explant image. For details of the first and third steps, see *SI Text*.

Two distinct mechanisms were used for generating neurite trajectories. The turning mechanism assumes that neurites respond to an imposed gradient by making small turns in their direction of growth, biased in the direction of the gradient (although subject to random noise), and growth rate remains constant. The growth-rate mechanism assumes that rate of neurite growth is modulated by the gradient, and the probability of turning up or down the gradient remains unbiased. We briefly summarize these mechanisms below. To mimic the experimental condition that neurites growing in a 3D medium tend to move in and out of the plane of focus, we simulated the *z*-coordinate of the neurite trajectory with a persistent random walk uncoupled to the *x* and *y* coordinates.

Turning Mechanism. At each timestep, the neurite moves a set distance in the direction it is currently heading. It then makes a small turn of magnitude $\delta\theta = \pi/30$ to the left or right. The presence of the gradient biases this choice, and we modeled this bias by assuming that the growth cone detects the change in concentration across its width, with a measurement whose SNR is related to the background concentration γ, gradient steepness μ, gradient direction θ_{NGF}, and the growth cone current direction θ according to

$$\mathrm{SNR} \propto \mu \sqrt{\frac{\gamma}{(1+\gamma)^3}} \sin(\theta - \theta_{NGF}). \quad [1]$$

(see ref. 11). In other words, to decide whether the growth cone turns left or right, we sampled from a Gaussian distribution $\mathcal{N}(\mathrm{SNR}, 1)$ with mean given by Eq. **1** and variance 1. If the sign of this quantity was positive, the growth cone turned right, and if it was negative, the growth cone turned left.

Growth-Rate Mechanism. In the growth-rate mechanism, at each timestep the neurite moves a variable distance in the direction it is currently heading. It then makes a small turn $\delta\theta = \pi/30$ to the right or left, selected in an unbiased manner. The gradient influences the neurite trajectory only through modulation of its growth rate. As with the turning mechanism, the growth rate is modulated in proportion to a measurement, with the SNR related to the gradient parameters., In this case, however, the measurement is made along the length of the growth cone, rather than across its width:

$$\mathrm{SNR} \propto \mu \sqrt{\frac{\gamma}{(1+\gamma)^3}} \cos(\theta - \theta_{NGF}). \quad [2]$$

The length of the step taken then is determined by multiplying the average step size by a factor $1 + k*\mathcal{N}(\mathrm{SNR}, 1)$, where *k* was set empirically to 0.5. The distance over which the comparison is made is encoded by μ, the fractional change in concentration over that distance. Thus, for example, the SNR will be much larger if the comparison is between the growth cone and the soma rather than just across the spatial extent of the growth cone.

Pipette Assay in 2D. SCGs were isolated by microdissection from postnatal day 1 (P1)–P3 Wistar rat pups (29). The SCGs were cut into thirds and incubated in Hanks' solution containing 0.25% trypsin at 37 °C for 20 min and then were gently triturated through flamed-polished Pasteur pipettes for 10 min to dissociate individual cells. The cells were plated in Opti-MEM solution containing 10 μg/mL laminin and 0.2 nM NGF on 35-mm Petri dishes and incubated overnight at 37 °C.

The assays were carried out on a heated microscope stage (Fryer Co.) at 37 °C to maintain the neurons at a native, biologically relevant temperature. Growth cones with a straight trailing axon of more than 20 μm of were selected for the assay. Gradients were generated using the pulsatile ejection method reported previously (12, 30). Briefly, a PV820 Pneumatic PicoPump (World Precision Instruments) and purpose-built electronic pulse stimulator was used to create a pressure of 5 psi with an electronically gated pulsatile frequency of 2 Hz and pulse duration of 50 ms. The NGF solution was applied to the axon through a micropipette with an average tip diameter of 1.3 μm (glass capillary pulled by a micropipette puller; Sutter Instrument) at a distance of 100 μm away from the growth cone. For Fig. 4 *A* and *B*, the pipette was positioned at 45° to the initial direction of growth of the neurite tip. For Fig. 4 *C* and *D*, the pipette was positioned at 0° ("in front") or 180° ("behind") to the initial direction of growth of the neurite tip. To monitor the chemical gradient produced, 70-kDa dextran labeled with fluorescent tetramethylrhodamine (Molecular Probes Inc) was added to the pipette solution.

A layer of prewarmed mineral oil was added gently to the top of the culture medium before assaying to prevent atmospheric exchange lowering the pH and to reduce evaporation. Images of the growing axon were taken using the 20× objective of a Nikon Eclipse TE200 inverted microscope at 60-s intervals for 1 h using a Q-Imaging camera and Q-Capture Pro software (Quantitative Imaging , Inc). Images were saved as .avi files.

Custom Matlab code was used to trace the path of each axon and to calculate the turning angle and distance of neurite outgrowth. The pipette location, initial direction of growth, and center of the growth cone were identified in the first frame of the movie, and then the center of the growth cone was located in each subsequent frame. The turning angle was defined as the angle between the original direction of growth and the average position of the growth cone in the last five frames in the trace. Plots tracing the paths of neurite growth for each condition also were generated automatically. The cumulative distributions of turning angles for each condition were compared statistically using the two-sample Kolmogorov-Smirnov test. Only growth cones with more than 15 μm of net growth over the period of the assay were included in the analysis.

Pipette Assay in 3D Collagen. Dissociated SCG neurons were labeled with pCAGYFP plasmid using an Amaxa nucelofector. After nucleofection, cells were resuspended in 0.2% collagen (as for the printing assay above), and a layer of collagen ≈100 μm thick was spread onto 35-mm glass-bottomed culture dishes

(MatTek). After gelling, the collagen was overlaid with 2 mL of Opti-MEM containing 0.3 nM NGF, and cells were grown overnight in a 37 °C, 5% CO_2 incubator. Neurites at least 50 μm long were positioned ≈100 μm from a micropipette filled with 1 μM NGF placed at 45° to the direction of growth of the neurite. NGF was ejected as per the 2D assay described above. While the plate was maintained at 37 °C and with a 5% CO_2 atmosphere, a 40-μm confocal z-stack (with a 4-μm interslice spacing) was acquired at 1-min intervals for 3 h using a Zeiss 5 Live microscope. Neurites that grew more than 20 μm in the horizontal plane and less than 20 μm in the vertical plane were analyzed as for the 2D assay described above using compressed z-stack .avi files.

ACKNOWLEDGMENTS. We thank E. Scott, L. Richards, and M. Hilliard for stimulating discussions and C. Haines for help with the human-scored turning analysis. Funding comes from an Australian Postgraduate Award (D.M.), Program Grant RPG0029/2008-C from the Human Frontier Science Program, Discovery Grant DP0666126 from the Australian Research Council, and Project Grant 456003 from the Australian National Health and Medical Research Council.

1. Yaron A, Zheng B (2007) Navigating their way to the clinic: Emerging roles for axon guidance molecules in neurological disorders and injury. *Dev Neurobiol* 67:1216–1231.
2. Lin L, Lesnick TG, Maraganore DM, Isacson O (2009) Axon guidance and synaptic maintenance: Preclinical markers for neurodegenerative disease and therapeutics. *Trends Neurosci* 32: 142–149.
3. Tessier-Lavigne M, Goodman CS (1996) The molecular biology of axon guidance. *Science* 274:1123–1133.
4. Dickson BJ (2002) Molecular mechanisms of axon guidance. *Science* 298:1959–1964.
5. Guan KL, Rao Y (2003) Signalling mechanisms mediating neuronal responses to guidance cues. *Nat Rev Neurosci* 4:941–956.
6. Huber AB, Kolodkin AL, Ginty DD, Cloutier JF (2003) Signaling at the growth cone: Ligand-receptor complexes and the control of axon growth and guidance. *Annu Rev Neurosci* 26:509–563.
7. Plachez C, Richards LJ (2005) Mechanisms of axon guidance in the developing nervous system. *Curr Top Dev Biol* 69:267–346.
8. Mortimer D, Fothergill T, Pujic Z, Richards LJ, Goodhill GJ (2008) Growth cone chemotaxis. *Trends Neurosci* 31:90–98.
9. Mortimer D, Goodhill GJ (2009) Axonal pathfinding. *Encylopedia of Neuroscience*, ed Squire LR (Academic, Oxford, UK), Vol 1, pp 1133–1138.
10. Lowery LA, Van Vactor D (2009) The trip of the tip: Understanding the growth cone machinery. *Nat Rev Mol Cell Biol* 10:332–343.
11. Mortimer D, et al. (2009) Bayesian model predicts the response of axons to molecular gradients. *Proc Natl Acad Sci USA* 106:10296–10301.
12. Lohof AM, Quillan M, Dan Y, Poo M-M (1992) Asymmetric modulation of cytosolic cAMP activity induces growth cone turning. *J Neurosci* 12:1253–1261.
13. Zheng JQ, Felder M, Connor JA, Poo M-M (1994) Turning of nerve growth cones induced by neurotransmitters. *Nature* 368:140–144.
14. Song HJ, Ming GL, Poo M-M (1997) cAMP-induced switching in turning direction of nerve growth cones. *Nature* 388:275–279.
15. Dertinger SK, Jiang X, Li Z, Murthy VN, Whitesides GM (2002) Gradients of substrate-bound laminin orient axonal specification of neurons. *Proc Natl Acad Sci USA* 99: 12542–12547.
16. Yam PT, Langlois SD, Morin S, Charron F (2009) Sonic hedgehog guides axons through a noncanonical, Src-family-kinase-dependent signaling pathway. *Neuron* 62:349–362.
17. Mai J, Fok L, Gao H, Zhang X, Poo M-M (2009) Axon initiation and growth cone turning on bound protein gradients. *J Neurosci* 29:7450–7458.
18. Lumsden AGS, Davies AM (1983) Earliest sensory nerve fibres are guided to peripheral targets by attractants other than nerve growth factor. *Nature* 306:786–788.
19. Lumsden AG, Davies AM (1986) Chemotropic effect of specific target epithelium in the developing mammalian nervous system. *Nature* 323:538–539.
20. Brose K, et al. (1999) Slit proteins bind Robo receptors and have an evolutionarily conserved role in repulsive axon guidance. *Cell* 96:795–806.
21. Meijering E, et al. (2004) Design and validation of a tool for neurite tracing and analysis in fluorescence microscopy images. *Cytometry A* 58:167–176.
22. Rosoff WJ, et al. (2004) A new chemotaxis assay shows the extreme sensitivity of axons to molecular gradients. *Nat Neurosci* 7:678–682.
23. Serafini T, et al. (1994) The netrins define a family of axon outgrowth-promoting proteins homologous to *C. elegans* UNC-6. *Cell* 78:409–424.
24. Bagnard D, Thomasset N, Lohrum M, Püschel AW, Bolz J (2000) Spatial distributions of guidance molecules regulate chemorepulsion and chemoattraction of growth cones. *J Neurosci* 20:1030–1035.
25. McLaughlin T, Hindges R, Yates PA, O'Leary DD (2003) Bifunctional action of ephrin-B1 as a repellent and attractant to control bidirectional branch extension in dorsal-ventral retinotopic mapping. *Development* 130:2407–2418.
26. Hansen MJ, Dallal GE, Flanagan JG (2004) Retinal axon response to ephrin-as shows a graded, concentration-dependent transition from growth promotion to inhibition. *Neuron* 42:717–730.
27. Bray D (1979) Mechanical tension produced by nerve cells in tissue culture. *J Cell Sci* 37:391–410.
28. Freeman WT, Adelson EH (1991) The design and use of steerable filters. *IEEE Trans Pattern Anal Mach Intell* 13:891–906.
29. Higgins D, Lein P, Osterhout D, Johnson MI (1991) Tissue culture of autonomic neurons. *Culturing Nerve Cells*, eds Banker G, Goslin K (MIT Press, Cambridge, MA), 1st Ed, pp 177–205.
30. Pujic Z, Giacomantonio CE, Unni D, Rosoff WJ, Goodhill GJ (2008) Analysis of the growth cone turning assay for studying axon guidance. *J Neurosci Methods* 170:220–228.